A STATISTICAL MODEL FOR THE FLUCTUATION OF SOUND TRANSMISSION IN THE SEA

R. J. Urick

Naval Surface Weapons Center,
White Oak Laboratory
Silver Spring, Maryland

11 February 1975

UNCLASSIFIED

SECURITY CLASSIFICATION OF THIS PAGE *(When Data Entered)*

REPORT DOCUMENTATION PAGE		READ INSTRUCTIONS BEFORE COMPLETING FORM
1. REPORT NUMBER NSWC/WOL/TR 75-18	2. GOVT ACCESSION NO.	3. RECIPIENT'S CATALOG NUMBER AD-A007 570
4. TITLE *(and Subtitle)* A Statistical Model for the Fluctuation of Sound Transmission in the Sea		5. TYPE OF REPORT & PERIOD COVERED Final 6. PERFORMING ORG. REPORT NUMBER
7. AUTHOR(s) R. J. URICK		8. CONTRACT OR GRANT NUMBER(s) A370-370A/WF11-121-707 Problem 202
9. PERFORMING ORGANIZATION NAME AND ADDRESS Naval Surface Weapons Center White Oak, Silver Spring, MD 20910 Acoustics Division, Code 221		10. PROGRAM ELEMENT, PROJECT, TASK AREA & WORK UNIT NUMBERS
11. CONTROLLING OFFICE NAME AND ADDRESS		12. REPORT DATE 11 February 1975 13. NUMBER OF PAGES 41
14. MONITORING AGENCY NAME & ADDRESS *(if different from Controlling Office)*		15. SECURITY CLASS. *(of this report)* UNCLASSIFIED 15a. DECLASSIFICATION/DOWNGRADING SCHEDULE

16. DISTRIBUTION STATEMENT *(of this Report)*

Approved for public release; distribution unlimited

17. DISTRIBUTION STATEMENT *(of the abstract entered in Block 20, if different from Report)*

18. SUPPLEMENTARY NOTES

19. KEY WORDS *(Continue on reverse side if necessary and identify by block number)*

Fluctuation
Propagation
Underwater Sound
Sound Transmissions
Signals
Sea

20. ABSTRACT *(Continue on reverse side if necessary and identify by block number)*

The fluctuations in amplitude of a narrow-band signal in the sea obey a simple mathematical relationship. Under the premise that fluctuations are caused by random multi-path contamination of an otherwise steady signal, it follows that they are distributed in amplitude in the same way as is the resultant of a constant vector plus the random vector representing the sum of the various multipath contributions. This distribution function was obtained many years ago by S. O. Rice and is sometimes called the

DD FORM 1 JAN 73 1473 EDITION OF 1 NOV 65 IS OBSOLETE
S/N 0102-014-6601

PRICES SUBJECT TO CHANGE

UNCLASSIFIED

SECURITY CLASSIFICATION OF THIS PAGE *(When Data Entered)*

Rician distribution. It can be represented by a family of curves having as a parameter the relative power in the multipath additions.

In this report the validity of this distribution for real signals in the sea is demonstrated by examples of fluctuations observed under a wide range of frequencies and propagation conditions. If it is indeed valid, the model permits us to predict the fluctuations of a transmitted signal in the sea around its mean intensity better, in many circumstances, than we can predict the mean intensity itself.

Preface

(U) This report presents a model for the fluctuation of narrow-band acoustic signals in the sea. It appears to be validated by actual signal data for a wide variety of conditions of frequency range and propagation type. The report is a contribution to the general subject of variability in sonar, and will be of interest to those engaged in sonar performance prediction and systems analysis.

(U) The report is based on work done under Task No. A370-370A/WF11-121-707.

ROBERT WILLIAMSON II
Captain USN

John B. Wilcox

JOHN B. WILCOX
By direction

A STATISTICAL MODEL FOR THE FLUCTUATION OF SOUND TRANSMISSION IN THE SEA

R. J. Urick

INTRODUCTION

1. (U) The amplitude fluctuations of received underwater acoustic signals have been repeatedly studied over the years, and a fair-sized bibliography containing over 100 entries can be compiled (Reference 1). Amplitude fluctuations have been observed, and their causes have been identified, under a wide variety of conditions. They have been studied most notably at short ranges, high frequencies and direct-path propagation, where the effects of the temperature and turbulence microstructure of the sea have been repeatedly measured in the field and accounted for in theory. Yet, under other conditions little seems to be known about fluctuations from a quantitative, predictive standpoint; in the past, the statistics of signal fluctuations often have been ignored, or smoothed out, in the search for the mean or time-averaged transmission between a source and a receiver in the sea. Because of this quantitative neglect, we have been able to say relatively little about the magnitude of the fluctuations or their distribution in amplitude, even though this knowledge is requried for improved sonar prediction models and for the improvement generally of sonar systems operating in the real, fluctuating ocean environment.

2. (U) This report presents a statistical model for describing the distribution in amplitude of the envelope of the signal from a distant, steady narrow-band source. The model is based on the premise that fluctuations are the result of multipath contamination of an otherwise steady signal. The validity of the model will be verified by an examination of the fluctuations as they have been obtained by analysis or as reported in the literature under a variety of experimental and propagation conditions.

---

1. G. C. Gaunaurd, Categorized Bibliography of the Topic of Underwater Sound Transmission Fluctuations, NOLTR 73-176, 1973.

3. (U) The other important aspect of the overall problem is the time scale of the fluctuations, as expressed by the auto-correlation function or the spectrum of successive samples of the signal. An earlier report (Reference 2) obtained fluctuation spectra for bottom-bounce low-frequency propagation over the range 0.05-0.5 Hz (2-20 seconds), and concluded that in this relatively short period range the fluctuations were caused by the rough, moving sea surface. However, at longer periods, little or nothing is known about the time scale of the fluctuation of the signal from a moving source (the condition of prime sonar interest); it seems plausible that the time scale depends on the rate at which multipaths are caused to interfere by the motion of the source the medium, or both. This subject will, it is hoped, be the topic of a future report.

A FLUCTUATION MODEL

4. (U) As a general statement, we may say that the fluctuations of the signal from a steady distant source in the sea are caused by multipath propagation in an inhomogeneous moving medium. Some examples of the multipaths that come to mind are the refracted paths in ducts, the four paths involving one bottom encounter in bottom-bounce propagation, and the paths from scatterers in the body or on the boundaries of the sea. Some examples of inhomogeneities are the rough sea surface, the temperature and salinity microstructure, and the biological matter existing in the body of the sea. These various inhomogeneities are always in motion relative to each other and to the source or receiver, or both, because of currents, turbulences, and source or receiver motion relative to the medium.

5. (U) The result is that a received signal is likely to consist, in whole or in part, of a number of contributions of random and time-varying phase and amplitude. These random multipath contributions will be negligible near the source but, with increasing distance, will tend to overwhelm the steady, direct path component and produce, at a long enough range, a resultant consisting only of components of varying phase and amplitude. As an example, the propagation through random microstructure may be viewed conceptually as consisting of a steady, direct path component that decreases with range together with scattered or diffracted components that increase with range and eventually dominate the received signal. At any range, the resultant is the sum of a steady and a random component, with an amplitude distribution that depends only on the fraction of the total average power in the random component.

THEORY

6. (U) In a classic paper published in 1945 (Reference 3), S. O. Rice derived the distribution function of the envelope of a sine wave plus narrow-band Gaussian random noise. This is the same as the distribution of the sum of a constant vector and a random vector whose x and y coordinates are Gaussian time-functions. In his honor, this function is called the Rician Distribution.

---

2. R. J. Urick, Fluctuation Spectra of Signals Transmitted in the Sea and Their Meaning for Signal Detectability, NOLTR 74-156, 1974.

3. S. O. Rice, Mathematical Analysis of Random Noise, Bell Sys. Tech. Jour. 24, 46, 1945, Art. 3.10.

7. (U) Referring to Figure 1, let there be a constant vector of magnitude P and arbitrary phase angle Ψ, to which is added a number of vectors each of random phase and random amplitude. The resultant V has the components

$$X(t) = P \cos \Psi + x(t)$$

$$Y(t) = P \sin \Psi + y(t)$$

where x(t) and y(t) are Gaussian time-variables of zero mean and variance σ^2_x and σ^2_y, respectively. The cloud of random vectors surrounding the tip of constant vector represent the multipath or scattered contributions to the steady component; their sum, by itself, has the well-known Rayleigh amplitude distribution. Rice showed that the probability density of the magnitude of the resultant, $V = (X^2 + Y^2)^{1/2}$, when σ^2_x and σ^2_y are arbitrarily taken to be unity, is

$$p(V) = V \exp\left[-\left(\frac{V^2+P^2}{2}\right)\right] I_o(PV)$$

where $I_o(PV)$ is the modified Bessel function of argument PV. Tables of this function are available (Reference 4).

8. (U) When the constant component vanishes, (P=0), the result is

$$p(V) = V \exp\left(\frac{-V^2}{2}\right),$$

since I(0) = 1; this is the Rayleigh distribution for the magnitude of the resultant of a large number of vectors of random phase and random amplitude. At the other extreme, when the product PV >>1, $I_o(PV)$ can be replaced by its asymptotic expansion

$$I_o(PV) = e^{PV}(2\pi PV)^{-1/2}\left(1 + \frac{1}{8PV} + \ldots.\right)$$

and the probability density becomes

$$= \left(\frac{V}{2\pi P}\right)^{1/2} \exp\left[\frac{-(V-P)^2}{2}\right]$$

4. M. Abramowitz and I. Stegun (Eds.), Handbook of Mathematical Functions, U. S. Dept. Commerce Applied Math. Series 55, 1964, Sect. 9.

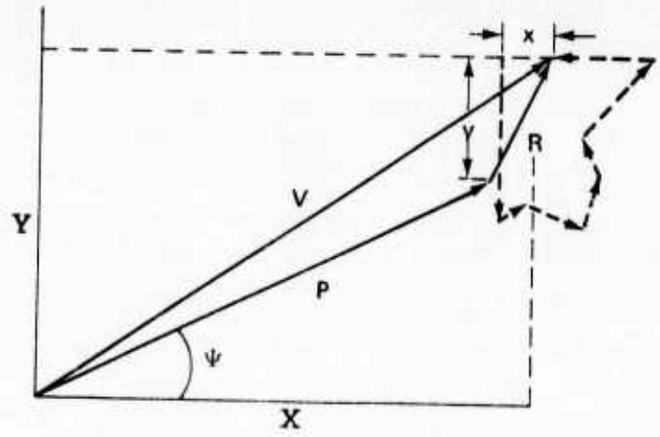

Figure 1. The resultant R of a number of random components is added to the constant vector P. Problem: find the amplitude distribution of the vectorial sum V.

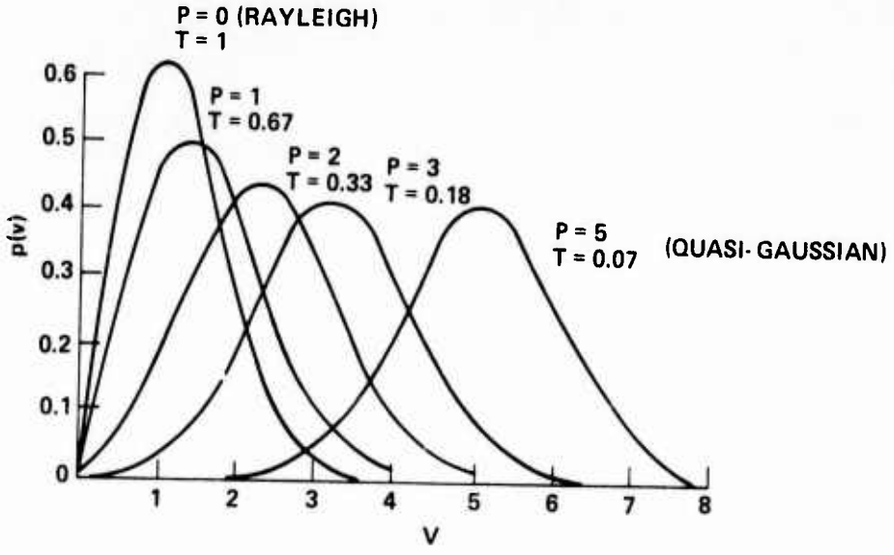

Figure 2. The Rician distribution for various values of P. The parameter T is the relative power in the random component of the signal.

This is the Gaussian distribution for unity standard deviation. It applies when either the magnitude of the constant vector P is large, or when V is far-out on the probability density curve, or both.

9. (U) Figure 2 shows the family of Rician distribution curves for several values of P as they were originally drawn by Rice. The curve for P=0 is the probability density curve of the Rayleigh distribution, while the curve for P=5 is sensibly Gaussian, except for V <<1.

10. (U) Figure 3 shows cumulative Rician distribution curves, giving the percentage of a large number of occurences in which the resultant V is equal to or less than the abscissa, expressed in units of $V^2/\overline{V^2}$. In acoustics, V is the equal signal amplitude, and the ratio $V^2/\overline{V^2}$ becomes equivalent to $I/\overline{I}$, the ratio of the signal intensity to the average intensity or mean square signal amplitude.

11. (U) With this ratio as the horizontal scale on semi-log paper, the Ravleigh distribution becomes a straight line, as seen in Figure 3. The parameter T used here is a measure of the relative randomness of the distribution, and is defined as the ratio of the random or Rayleigh power to the total power of the received signal. The ratio T, which may be called the randomness factor or randomicity is related to P by

$$T = \frac{\text{Rayleigh Power}}{\text{Total Power}} = \frac{2}{P^2+2}$$

inasmuch as the Rayleigh power is equal to $\sigma^2_x + \sigma^2_y = 1+1=2$. The randomicity T varies from zero for a completely constant signal ($P\to\infty$) to unity for a completely random signal (P=0) composed entirely of contributions of random phase and amplitude. The parameter T is equal to the square of the coefficient of variation of the distribution for small T or large P when the distribution is normal or Gaussian; when T=1, the coefficient of variation becomes that of the Rayleigh distribution which can be shown to equal to

$$\left[(4/\pi)-1\right]^{1/2} = 0.52.$$

12. (U) With a horizontal scale of decibels, and on a probability or Gaussian vertical scale, the cumulative Rician distribution curves become those of Figure 4. Two characteristics of this family of curves are noteworthy.

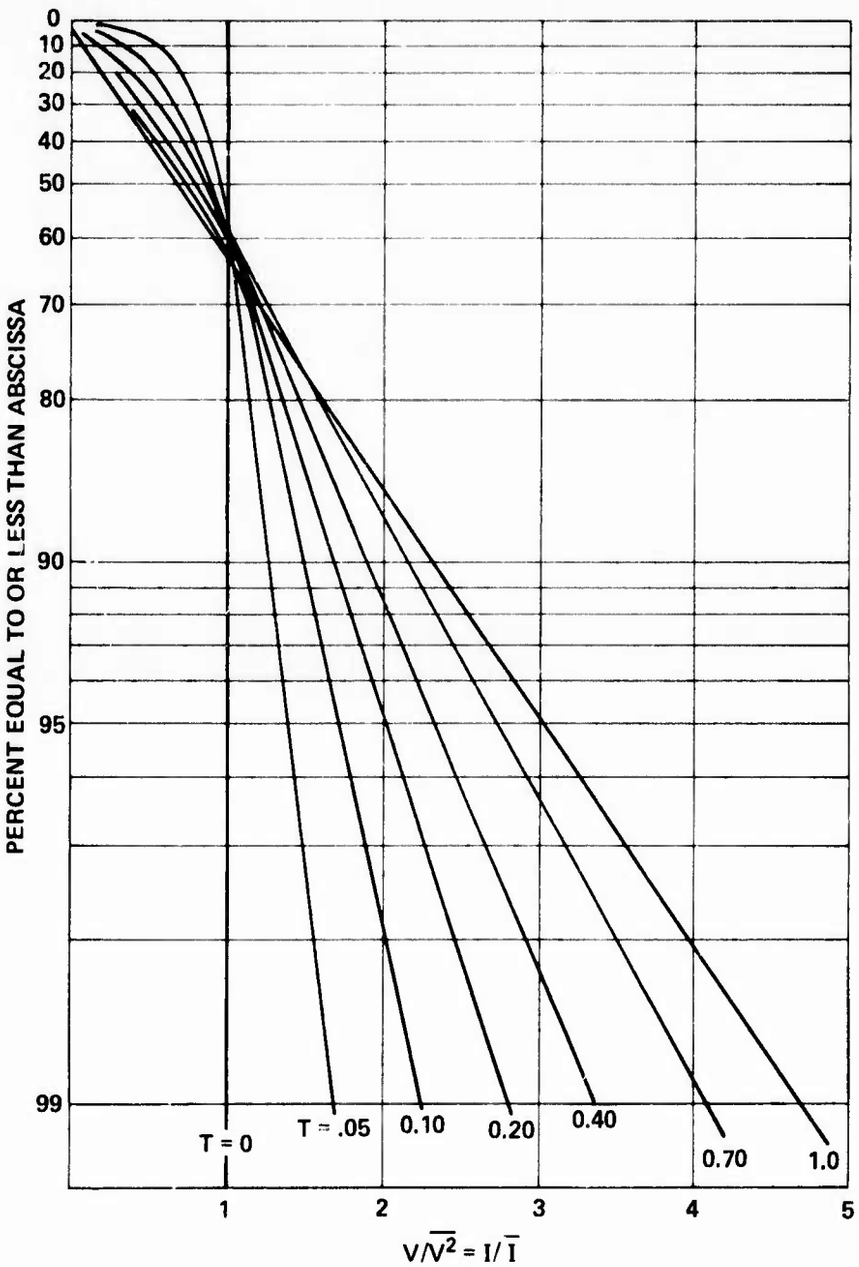

Figure 3. Rician curves with T as parameter on semi-log coordinates.

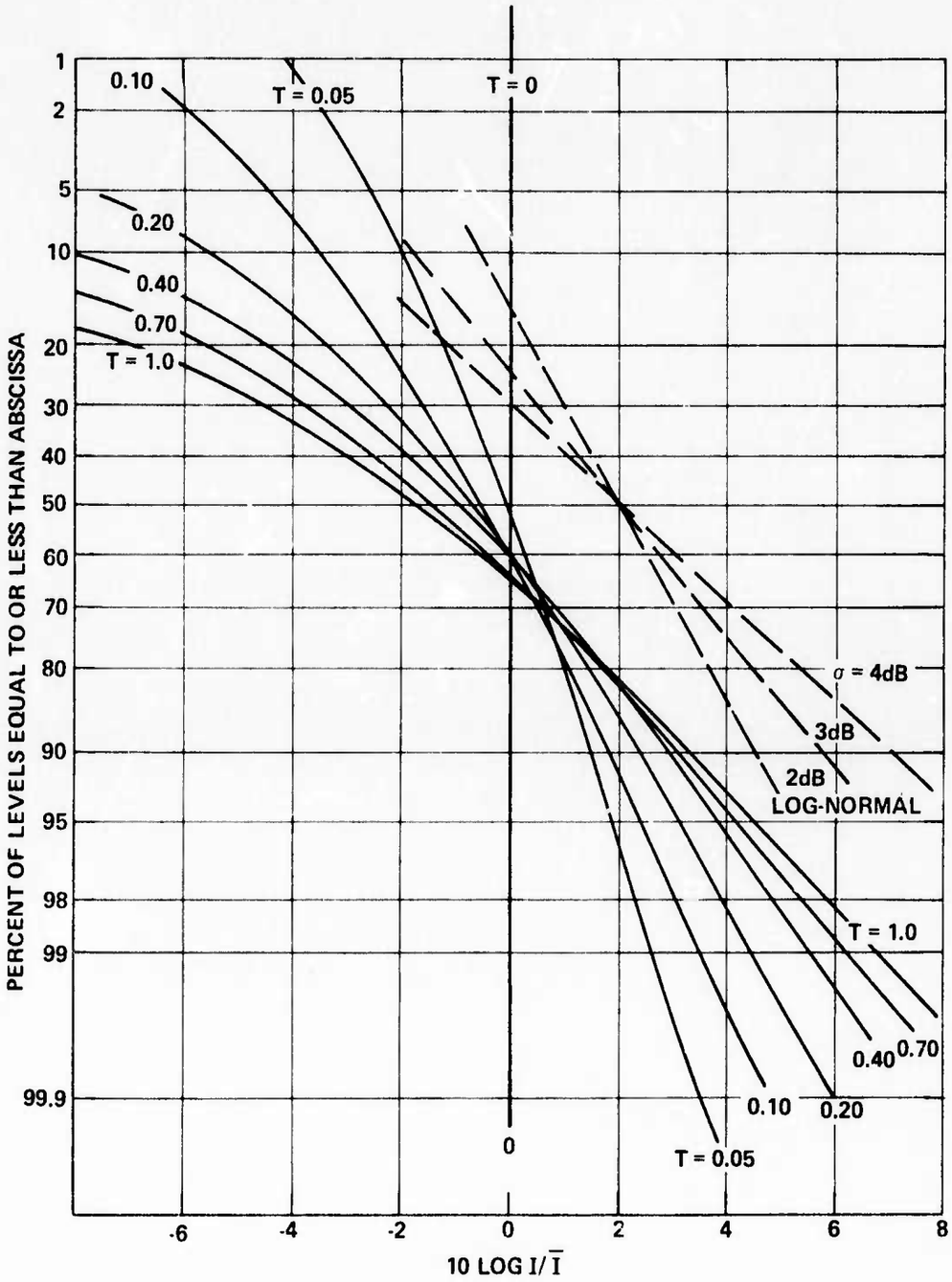

Figure 4. Rician curves with T as parameter on probability coordinates and a logarithmic horizontal scale.

First, the curves tend to be log-normal or straight lines for small T and/or for 10 log $I/\overline{I} > 1$. They depart from log-normality at the low end; there are more small signals than an extrapolation of the distribution of the high level quasi-log-normal signals would predict. Second, the curves are crowded together for the larger values of T; for T>0.5, the various distribution curves are nearly identical.

13. (U) Thus we arrive at the conclusion that, according to the present model, the distribution of intensities becomes sensibly the same whenever the multipath contributions become an appreciable fraction of the total received power. In short, signal intensities greater than the mean intensity tend to be log-normally distributed, with σ between 2 and 4 db, and tend toward the Rayleigh limit whenever random multipaths account for roughly more than half of the received power (i.e. T > 0.5).

MODEL VERIFICATION

14. (U) As a test of the validity of the model in the real world, a number of fluctuation examples have been examined. Some have resulted from digital analyses of tape recordings made at NAVSURFWPNCEN, while others are based on signal level readings taken from plots or graphical playouts published in the literature. These various examples are here called "cases." In each "case" the time interval over which the data extends is two hours or less, except in one case where the recorded data covered a half-day. Thus, long-period variables, such as these associated with long-term changes in the medium, are excluded. The intent is to present examples of fluctuations as they actually occur under a wide variety of conditions of frequency, range and propagation conditions and where the statistics are reasonably stationary, in order to see whether the multipath model is indeed valid under a majority of situations of practical sonar interest.

15. (U) The cases to follow apply for three major kinds of propagation: surface-duct, bottom-bounce, and long range refracted paths. They are presented in Figures 5 to 13 in three parts. Part (a) is a sketch showing the existing propagation paths for the particular case; part (b) is a sample of the variability being analyzed; part (c) gives the resulting distribution curves on a db scale, along with one or more of the curves of Figure 4 for comparison. Table I is a listing of the experimental conditions for each case, along with a reference number, keyed to the list of references in where more information may be found.

Case 1 (Figure 5)

16. (U) This example is based on a series of 100 pulses at 13.0 kHz. They were transmitted at 10 second intervals and were received by hydrophones located within and below a mixed layer 180 feet thick. Source and receivers were stationary. The pulse length was 0.1 second. A mean level was read for each pulse so that the integration time per data sample was also 0.1 second.

17. (U) The resulting distribution is seen from Figure 5c to be essentially Rayleigh, with T = 1.0. From a propagation standpoint this must mean that forward scattering, doubtless from the sea surface, is likely to have been the dominant transmission mechanism to a receiver located both in and below the layer.

Case 2 (Figure 6)

18. (U) Here surface duct propagation is also involved but with continuous-wave (CW) transmission at a lower frequency (1120 Hz). The source was towed at a speed of 5 knots, but the results were found to be the same when the source was stationary. Sanborn playouts of the received signal at two hydrophones in and below the surface duct were read off at 1 second intervals using an integration or smoothing time of about 1/4 sec.

19. (U) The distribution of 100 readings was found to be Rayleigh (T=1.0) below the duct, and to be fitted by the Rician distribution for T=0.1 within the duct. This finding is consistent with the view that a below-duct sensor receives only scattered sound, whereas the signal in the duct is dominated by a steady component containing only a small (10%) admixture of scattered sound.

Case 3 (Figure 7)

20. (U) In this example the receivers are well below the duct at depths of 1000 and 8000 feet. A ray diagram shows that the 8000 foot unit is within the direct sound field of the source, whereas the 1000 foot receiver is within the shadow below the duct so as to receive sound only via surface and volume scattering. The sea bottom is too deep (13,000 ft) and has too high a loss (about 10 db) to contribute appreciably to the received sound.

21. (U) The 1000 ft receiver is seen to receive a substantially Rayleigh distributed signal, just as for the below-duct receiver of Case 2. At 8000 ft the signal fluctuation is much less and corresponds to T = 0.2. Thus at 8000 ft the power in the constant component of the signal, according to our model, represents 80% of the total power. The remaining 20% must be due to scattering out of the surface duct from the deep scattering layer or from the microstructure below the duct.

Case 4 (Figure 8)

22. (U) This case involves surface-duct transmission at frequencies of 700, 1300, and 3000 kHz. The data point were read from figures given in a paper by H. Eden and J. Nicol in the Journal of the Acoustical Society of America (JASA). In this work pulses of unstated pulse length and repetition rate were transmitted from a moving source as it opened range between 4 and 32 kyds from a receiver located within a 200 ft surface duct.

23. The distribution of the points representing the received levels is seen to be nearly Rayleigh at 3000 Hz and to be fitted by the Rician curve for T = 0.1 at 700 Hz. This result is consistent with the findings of Cases 1 and 2 in that the fluctuation is found to decrease with decreasing frequency. At 700 Hz--a frequency still well-trapped in the 200 ft duct--the random power appears to represent only 10% of the total received signal power.

Case 5 (Figure 9)

24. (U) In this example the transmission is between a shallow source and a shallow receiver via bottom bounce paths. The CW transmission frequency of 142 Hz was too low to be trapped by the 120 ft surface duct. The towing speed of the source was 3 knots from a range of 11.2 to 29.3 ky. Data samples were obtained by digitizing a tape recording using integration times of 8, 16, and 128 sec; in addition, data points using an integration time of about 1/4 sec were obtained by reading at 1 sec intervals a Visicorder trace such as the one shown in Figure 9b.

25. (U) The distribution of levels at all integration times is found to be essentially the same. The data is fitted by the Rician curve corresponding to T = 0.2, except at the low end, where the deficiency of small values may possibly be due to noise contamination; that is, to an insufficient signal-to-noise ratio in the data.

Case 6 (Figure 11)

26. (U) This is also a low-frequency radial run, but from another field exercise. Here the received CW at 185 Hz was sampled at 1 minute intervals for a period of 1 hour, using a 10-second integration time. During the data period the source closed its range from 22ky to 8ky. The total number of samples was only 58.

27. (U) The distribution of these samples fits our model only crudely, falling between T = 0.4 and T = 1.0. There is a deficiency of high amplitude samples. If this is not a fault of the model, this deficiency may be the result of slight overloading in the recorded data.

Case 7 (Figure 10)

28. (U) This is the same field data as Case 6, but for a tangential run of the towed source past the receiver, with the closest-point of-approach occurring at a range of 19 ky. The analyzed data extends over a time period of slightly over 2 hours. A sampling interval of 10 sec and an integration time of 10 sec were used. The total number of the contiguous data samples was 740 on each of two passes of the towed source past the receiver.

29. (U) The distribution of these samples is fitted by the Rician curve for approximately T = 0.4, except for a deficiency of high amplitudes, as in the previous example involving the same recorded data.

Case 8 (Figure 12)

30. (U) This is an analysis of 100 plotted points taken from a British report of a transmission run made in 1300 fathoms of water with a negative gradient. These points are shown in Figure 12b, reproduced from the report. The superposed sloping sets of lines were drawn by eye to remove the effect of range; the fluctuations we are interested in are the deviations from this estimate of the mean transmission. Each plotted point was originally a level reading made at intervals from a playout of the recorded run. The integration time used was unstated, but apparently was short.

31. (U) This data shows reasonable agreement with the model, considering the crude manner used to obtain and measure the numerical data. The distribution is approximately Rayleigh, as a result, according to our model of transmission via bottom-bounce multipaths.

Case 9 (Figure 13)

32. (U) This case involves CW transmission during two 12-hour periods over refracted paths some 700 miles long between using a fixed source an Eleuthera and a fixed receiver at Bermuda. Data points were obtained by reading off values at regular intervals from traces of received signal level included in a progress report by J. Clark and M. Kronegold of the Institute of Acoustical Research, Miami, Florida. These traces are reproduced in Figure 12b; from the 143 and 98 values, respectively, were read by eye at the time intervals of the vertical lines. In this example the transmission is via numerous refracted and RSR paths that undergo numerous oscillations along the 700-mile transmission distance (Figure 13a).

33. (U) The distribution of the received levels is found to nearly Rayleigh in keeping with the existence of numerous ray path contributions to the received signal in a mobile and essentially random deep ocean medium. Turbulences and internal waves doubtless cause the refracted multipaths to vary constantly in phase and amplitude so as to result in a Rayleigh-distributed signal.

Case 10 (Figure 14)

34. (U) This case also pertains to transmission from Eleuthera to Bermuda at essentially the same frequency as Case 9. The data appears in a paper in JASA as histograms of the amplitude of the received signal (Figure 14b.) over a 3-hour period at two hydrophones 93 meters apart. The signal was sampled and integrated using a 15 second integration time.

35. (U) When converted to db, summed and normalized, the histograms become cumulative distributions that are substantially Rayleigh, through showing deviations at the low end that are likely to be significant because of the large number of data samples. This may be due to some degree of non-stationarity in the statistics. While the coefficient of variation was found, in the paper cited, to be close to the Rayleigh value (52%), the distribution was found by statistical tests described in the paper to be nearly Gaussian, rather than Rayleigh.

Case 11 (Figure 15)

36. (U) Here there was a single refracted path not reaching the sea surface between a deep source and a deep receiver 24 miles away. A 5 ms pulse at 800 Hz was transmitted every6 minutes over a 2 day period. Amplitudes were read off from a trace (Figure 15b.) given in a paper published by R. M. Kennedy in JASA. The use of short pulses and reading the amplitude of the first arrival effectively eliminated any widely diverging multipaths.

37. (U) This data is seen to follow the Rician curve for T = 0.2 reasonably well, although the number of data points (n = 82) is small. If interpreted as being log-normally distributed, the amplitudes would have a σ equal to 2.4 db; a value the same as that found in the published paper from an analysis of all the data obtained. In the present case, the randomness (amounting to 20% of the received power) is likely to have been caused by propagation through inhomogeneous water at shallow depths along the path from source to receiver.

DISCUSSION

38. (U) In the foregoing we have seen some examples of fluctuations that amount to no more than "snapshots" of the fluctuation existing under a variety of experimental and transmission conditions. Our purpose was to exercise the model for a broad sampling of situations of sonar interest, rather than to exhaustively analyze one particular set of data. All the cases that have been examined have been presented, without deletion of cases that do not validate the model. No data from ray trace or normal mode computations preserving phase--which always prominently display fluctuations as a function of range--have been used. The number of data samples has been small in most cases and the original data may have suffered from the maladies of noise contamination at low-levels and system nonlinearity at high levels.

39. (U) A proper validation of a fluctuation model requires a large number of samples from high quality recordings, in order that the tails of the distribution curves--where the real test of the model lies--can be elucidated. In conflict with this requirement for large sample sizes are the long integration times of interest to passive sonar, plus the requirement for statistical stationarity in the data--which means the absence of a long-term trend such as resulting from large changes in range or diurnal (or longer) changes in medium. These considerations greatly restrict the number of available data samples and enhance the difficulty of model validation. Nevertheless, what we have obtained in the foregoing is an indication, at least, that the model is useful for first-cut prediction of fluctuation whenever--as always the case--multipath propagation of some kind exists between source and receiver.

SUMMARY

40. (U) If we assume the validity of the model, we can make the following statements concerning the amplitude fluctuations of narrow-band underwater acoustic signals:

1. Amplitude fluctuations are caused by multipath contamination of an invariant propagation path and depend upon the fraction of the total received power contained in the multipaths.

2. When this random fraction is greater than 50%, the signal levels approach the Rayleigh distribution. No greater fluctuation than that represented by the Rayleigh distribution is possible.

3. The upper 40% or so of received signals are log-normally distributed, with a σ that lies between 2 and 4 db, depending on the admixture of multipaths in the propagation.

4. The median intensity of the signal population (level exceeded by 50% of the signal samples) lies 1 to 2db below the mean intensity (or mean-square signal amplitude).

5. Weak signals have a greater and more variable σ than do strong signals; in other words, there are more low level signal samples than the log-normal distribution of the strong signals would predict. Observations generally show (see, for example, Cases 3, 4, and 9 above) that a received signal is characterized by long periods of strong and slightly varying level interrupted by shorter periods of deep low-levels fades.

6. If our model is indeed valid, we may conclude, suprisingly, that the fluctuation statistics of a received signal often can be predicted more accurately than can the mean or time-averaged signal level itself.

7. In the foregoing, we have been concerned only with the changes in signal level received by a single distant receiver from a steady source. Many aspects of the overall fluctuations problem remain. As mentioned earlier, the time-scale of the fluctuations has not been studied, and neither have the fluctuations of amplitude and phase between separated hydrophones. Equally important and similarly unstudied are the fluctuations in the noise background and in the other sonar parameters. These matters--all of interest to the sonar analyst, performance predictor and designer--are matters for future investigation.

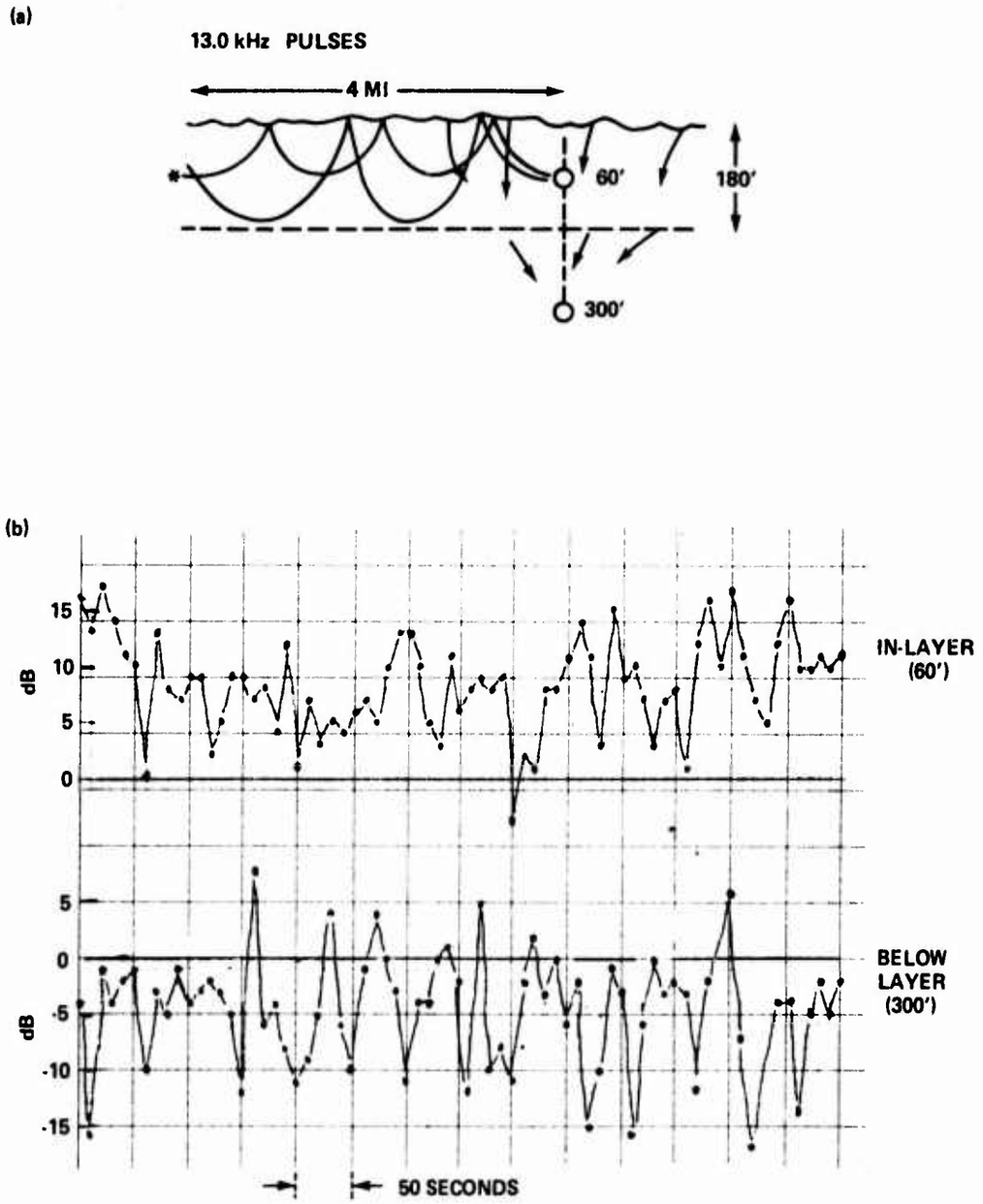

Figure 5a,b. Fluctuation example, Case 1.

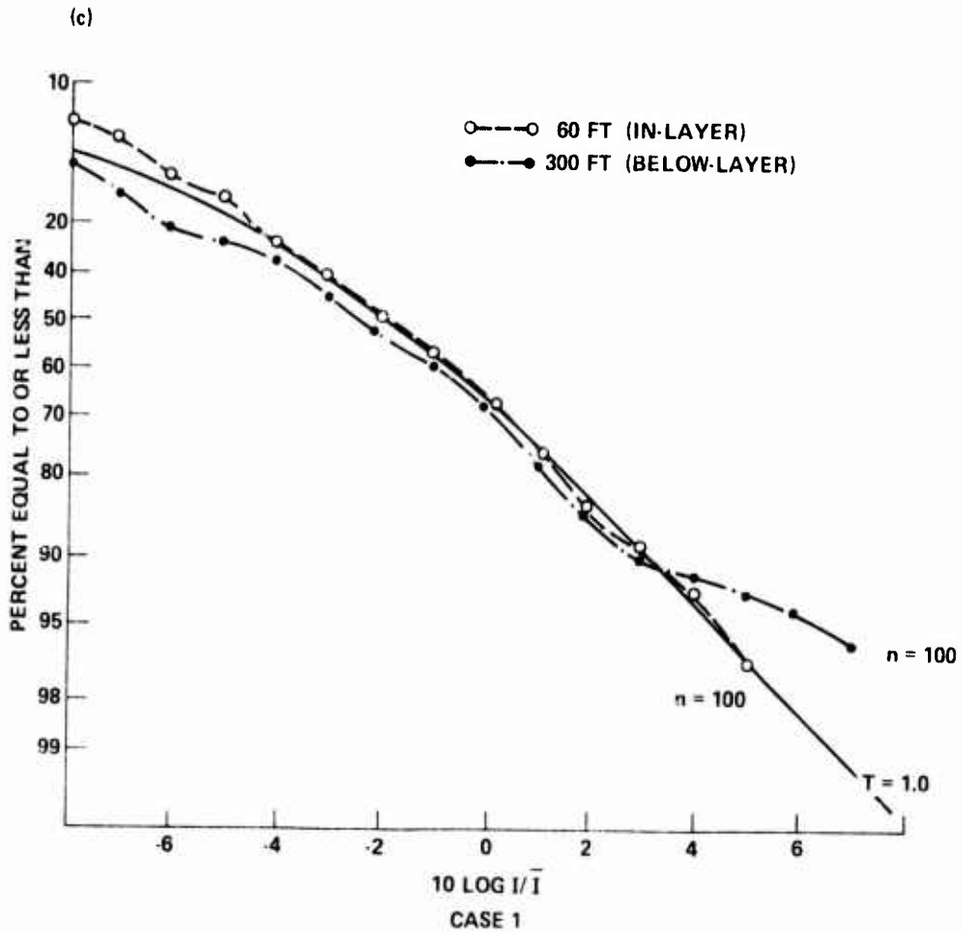

Figure 5c. Amplitude distribution, Case 1.

(a)

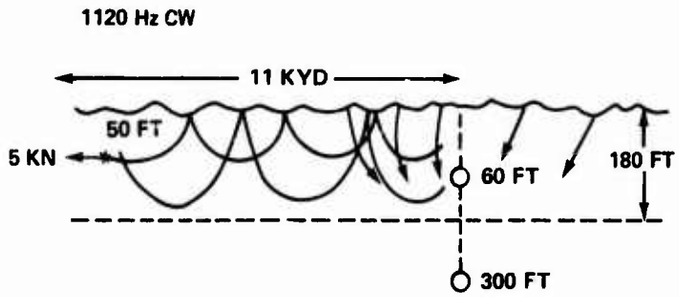

(b)

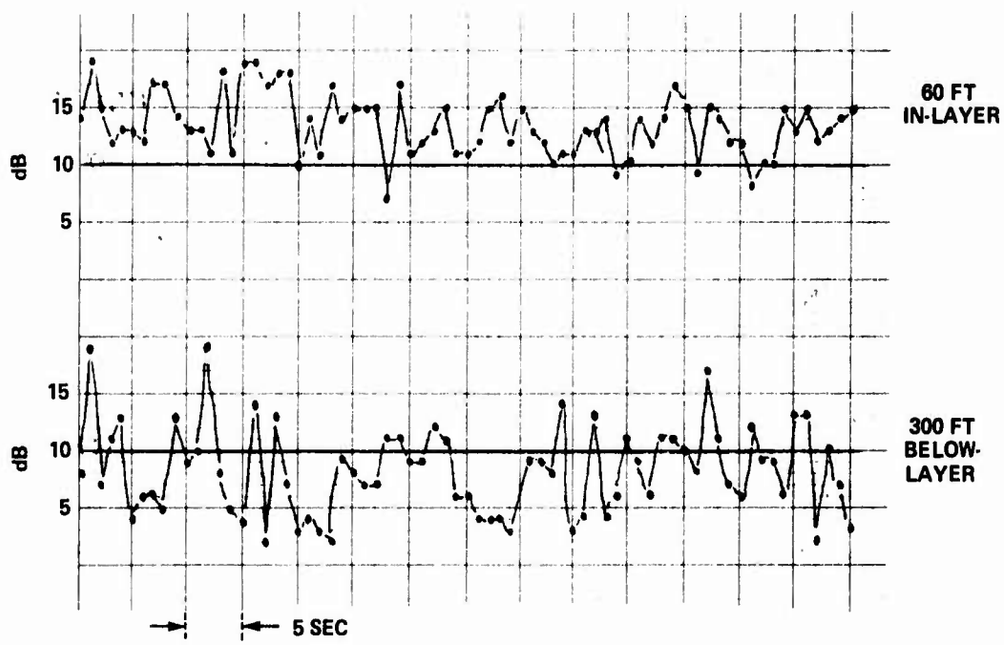

SAMPLING INTERVAL 1 SEC; INTEG TIME: APPROX ¼ SEC.

CASE 2

Figure 6a,b. Fluctuation example, Case 2.

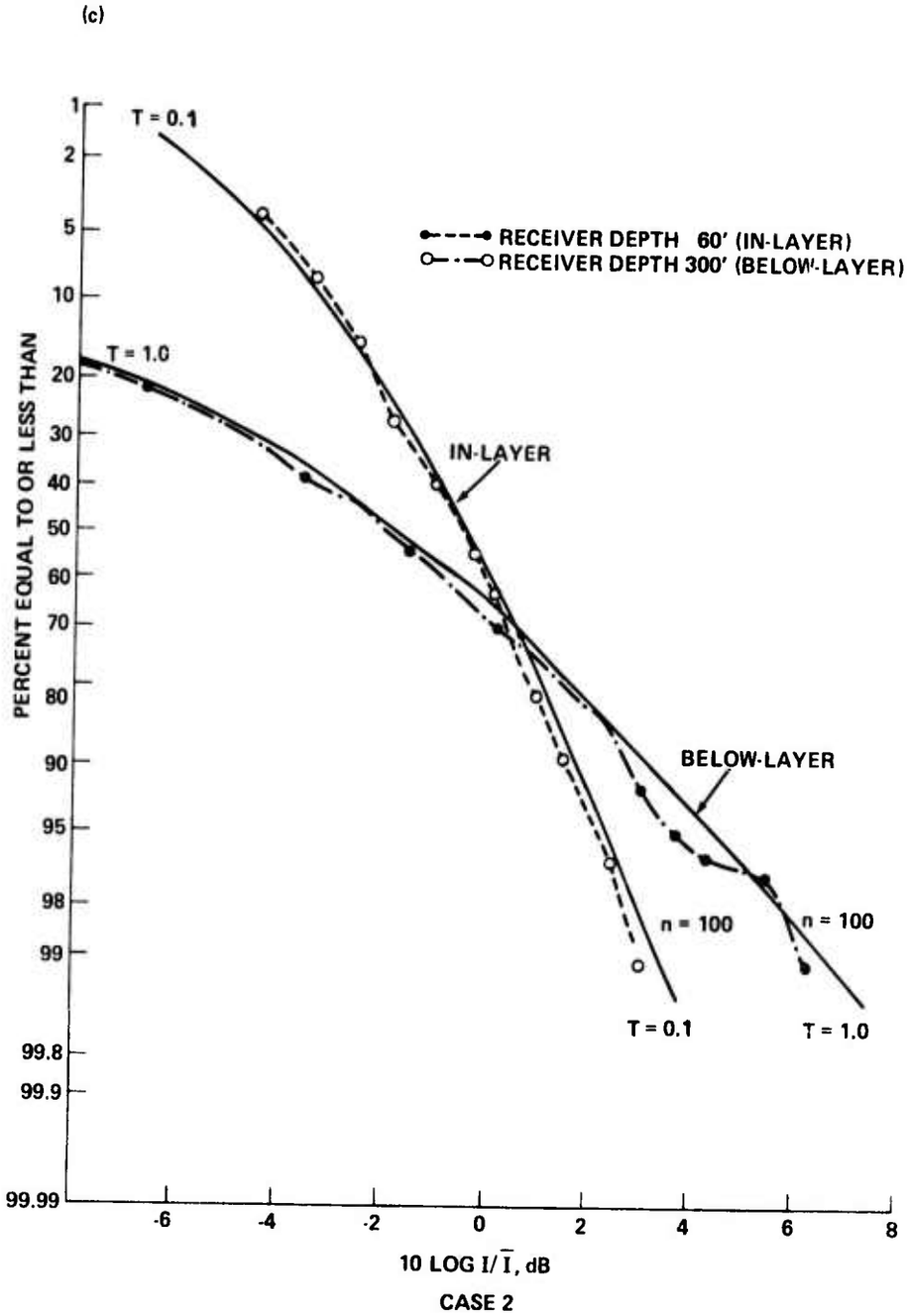

Figure 6c. Amplitude distribution, Case 2.

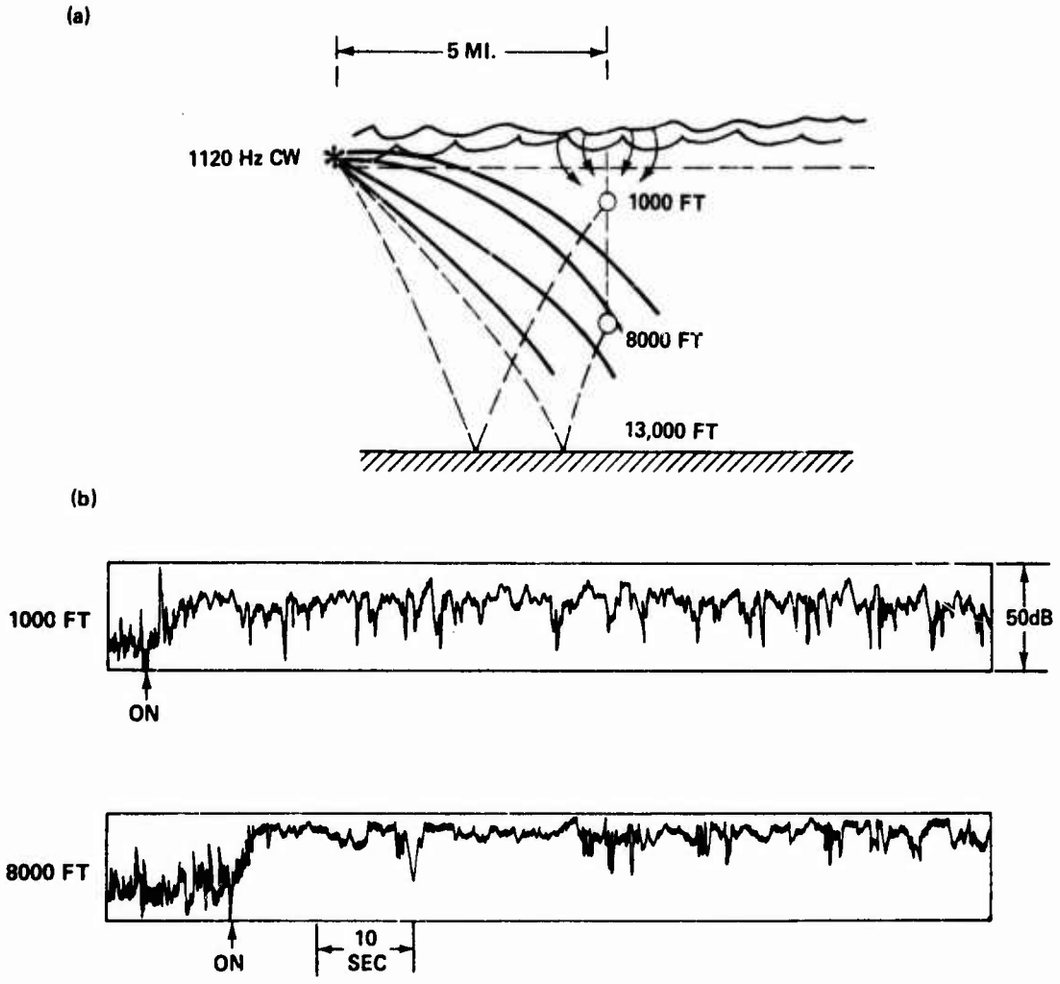

SAMPLING INTERVAL 1 SEC; INTEG TIME CA 0.1 SEC

CASE 3

Figure 7a,b. Fluctuation example, Case 3.

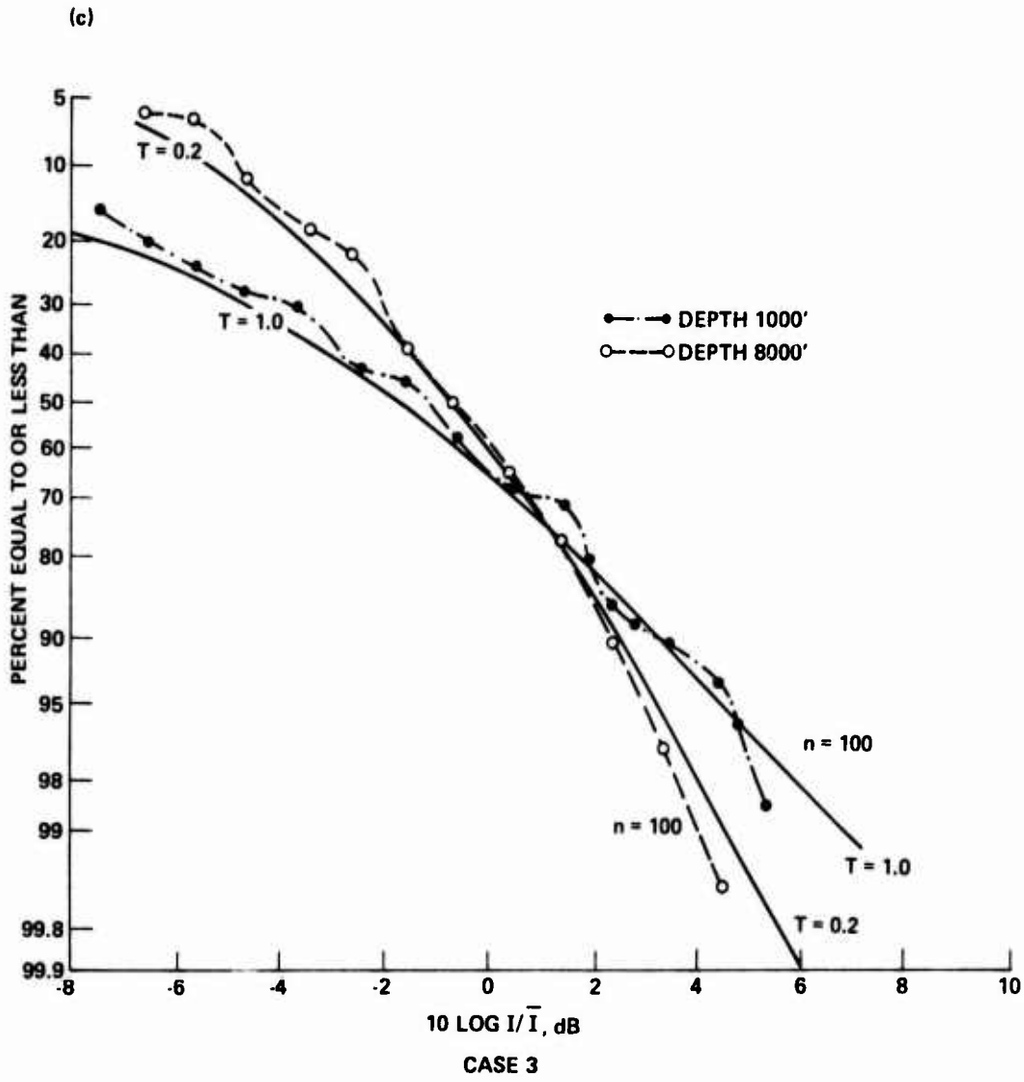

Figure 7c. Amplitude distribution, Case 3.

(a)

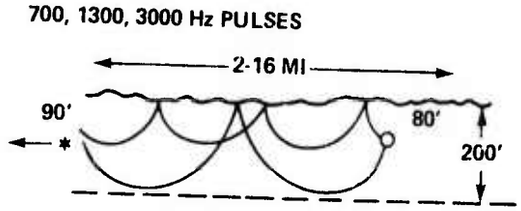

(b)

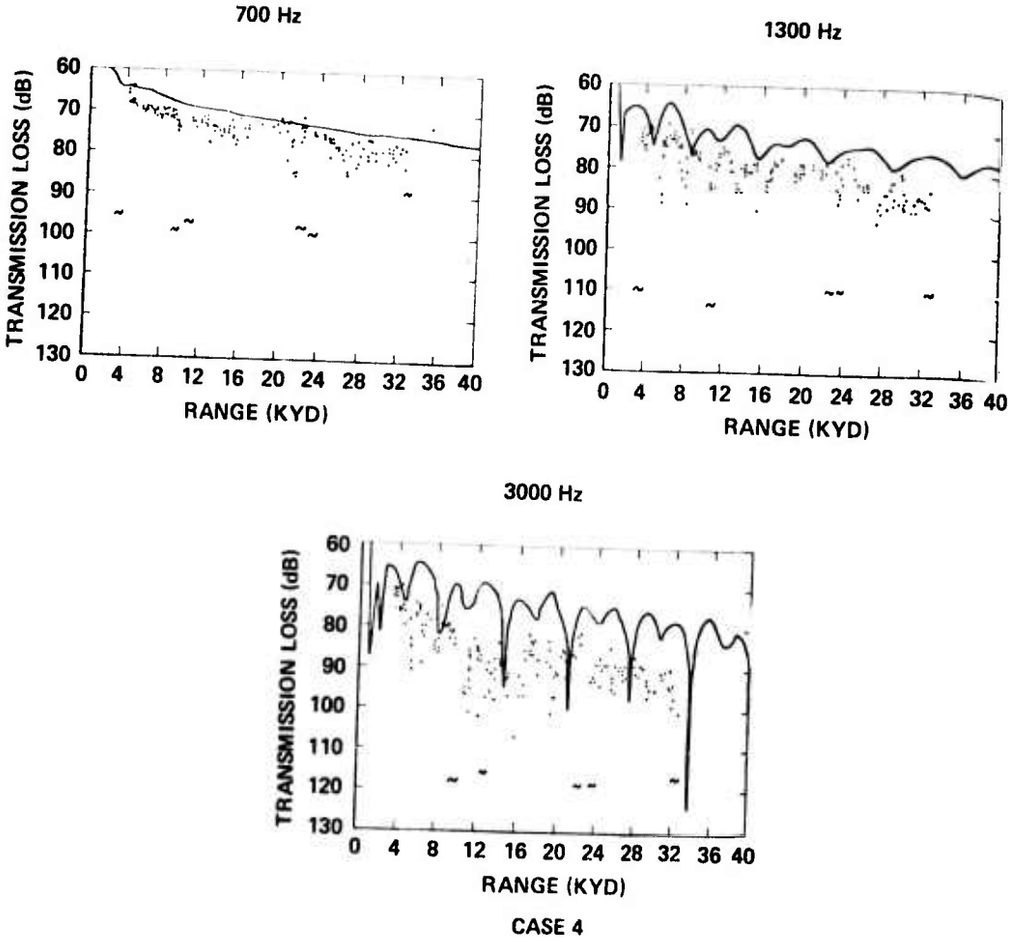

Figure 8a,b. Fluctuation example, Case 4.

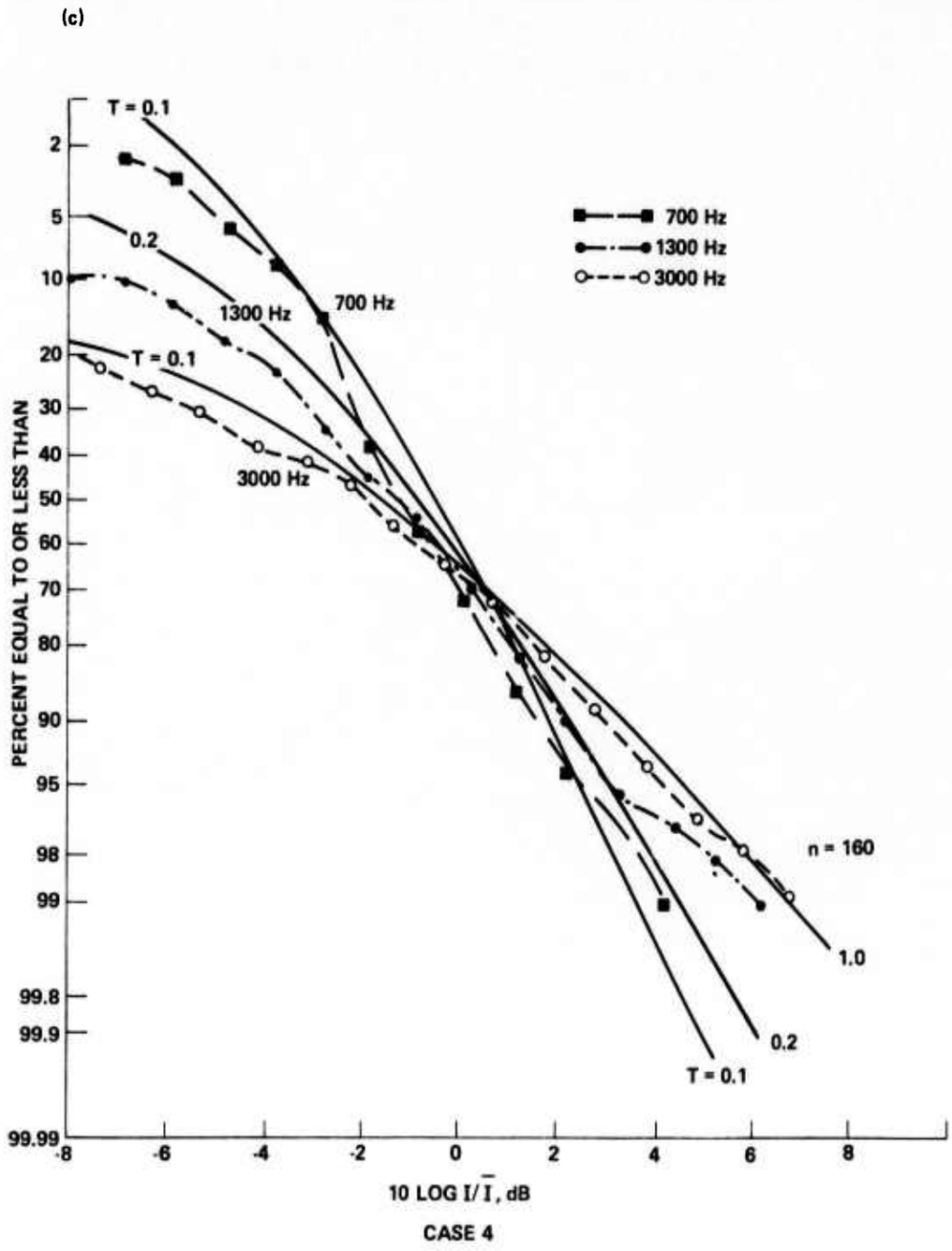

Figure 8c. Amplitude distribution, Case 4.

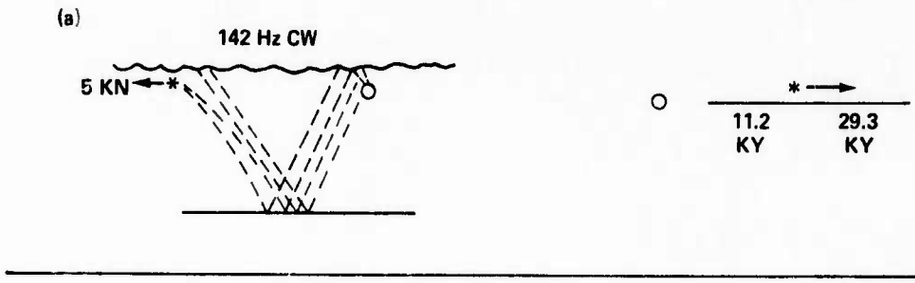

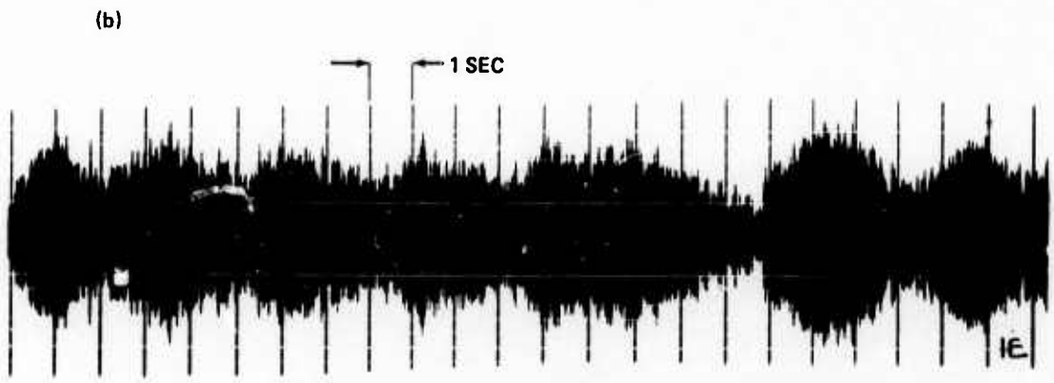

¼ SEC (EST) INTEGRATION TIME, SAMPLE INTERVAL 1 SEC (CODE IE 29.3 KY)

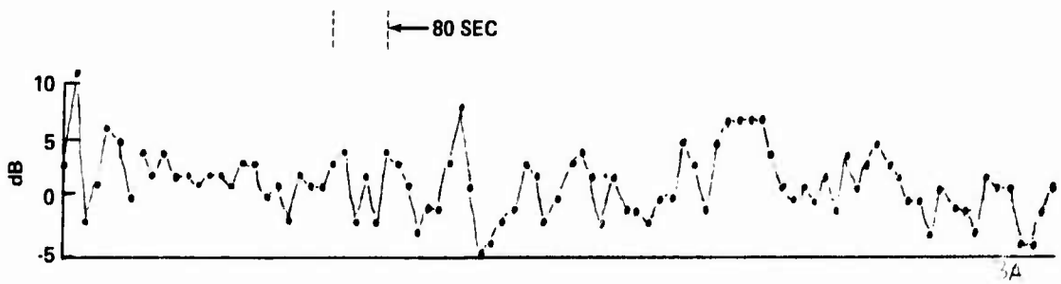

16 SEC INT TIME, SAMPLE INTERVAL: 16 SEC (CODE 3C 11.2-12.8 KY)

CASE 5

Figure 9a,b. Fluctuation example, Case 5.

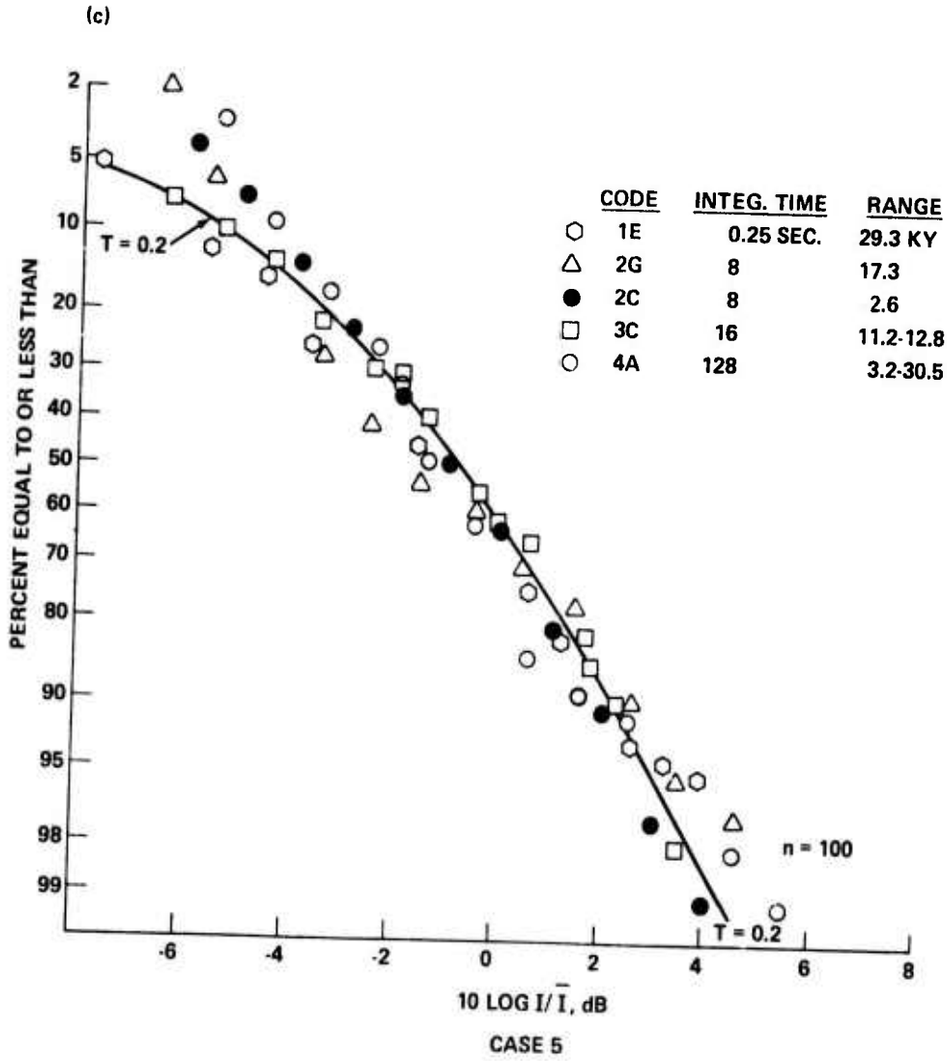

Figure 9c. Amplitude distribution, Case 5.

(a)

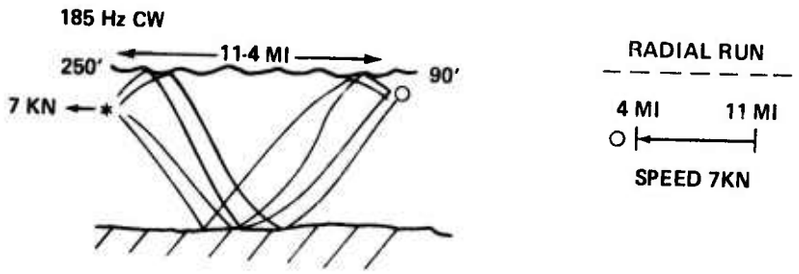

(b)

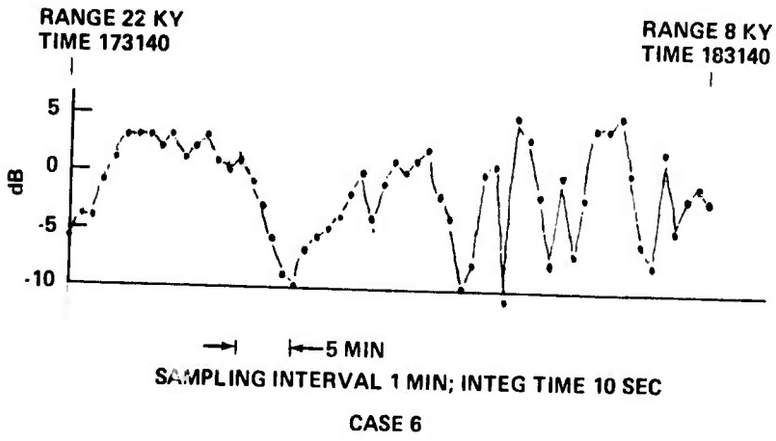

Figure 10a,b. Fluctuation example, Case 6.

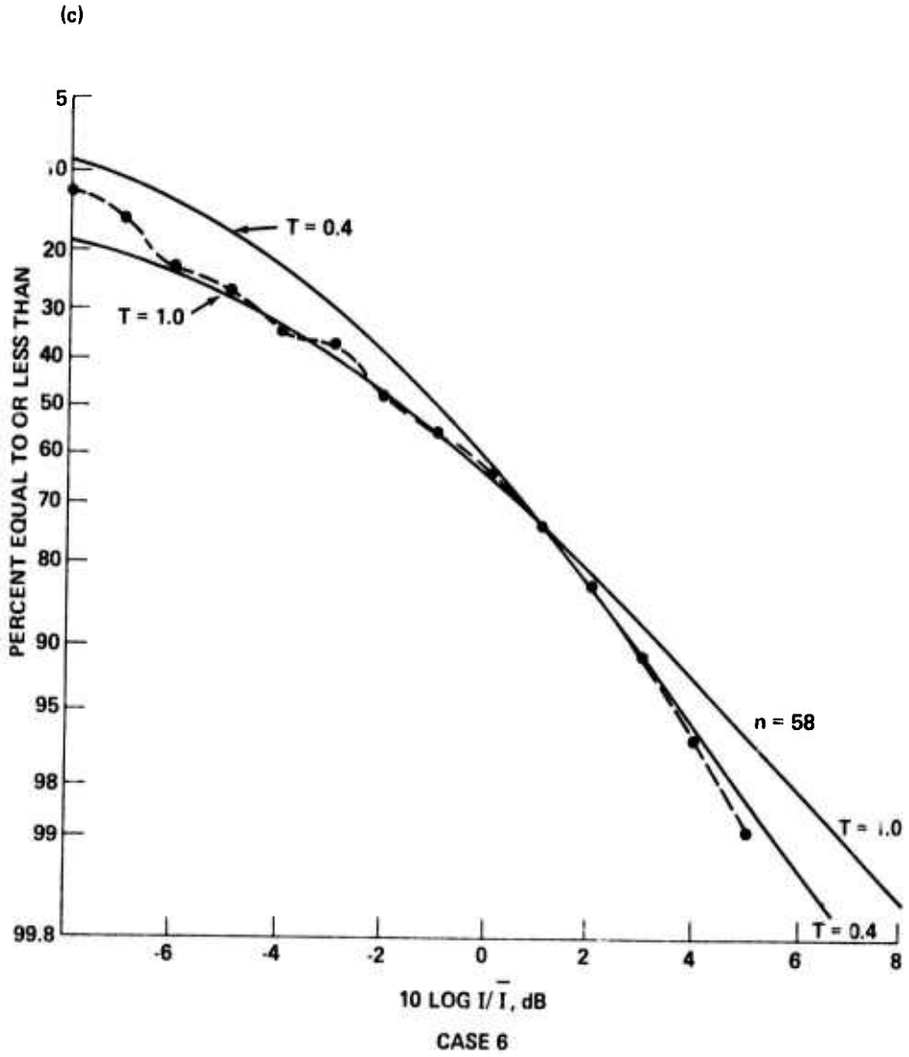

Figure 10c. Amplitude distribution, Case 6.

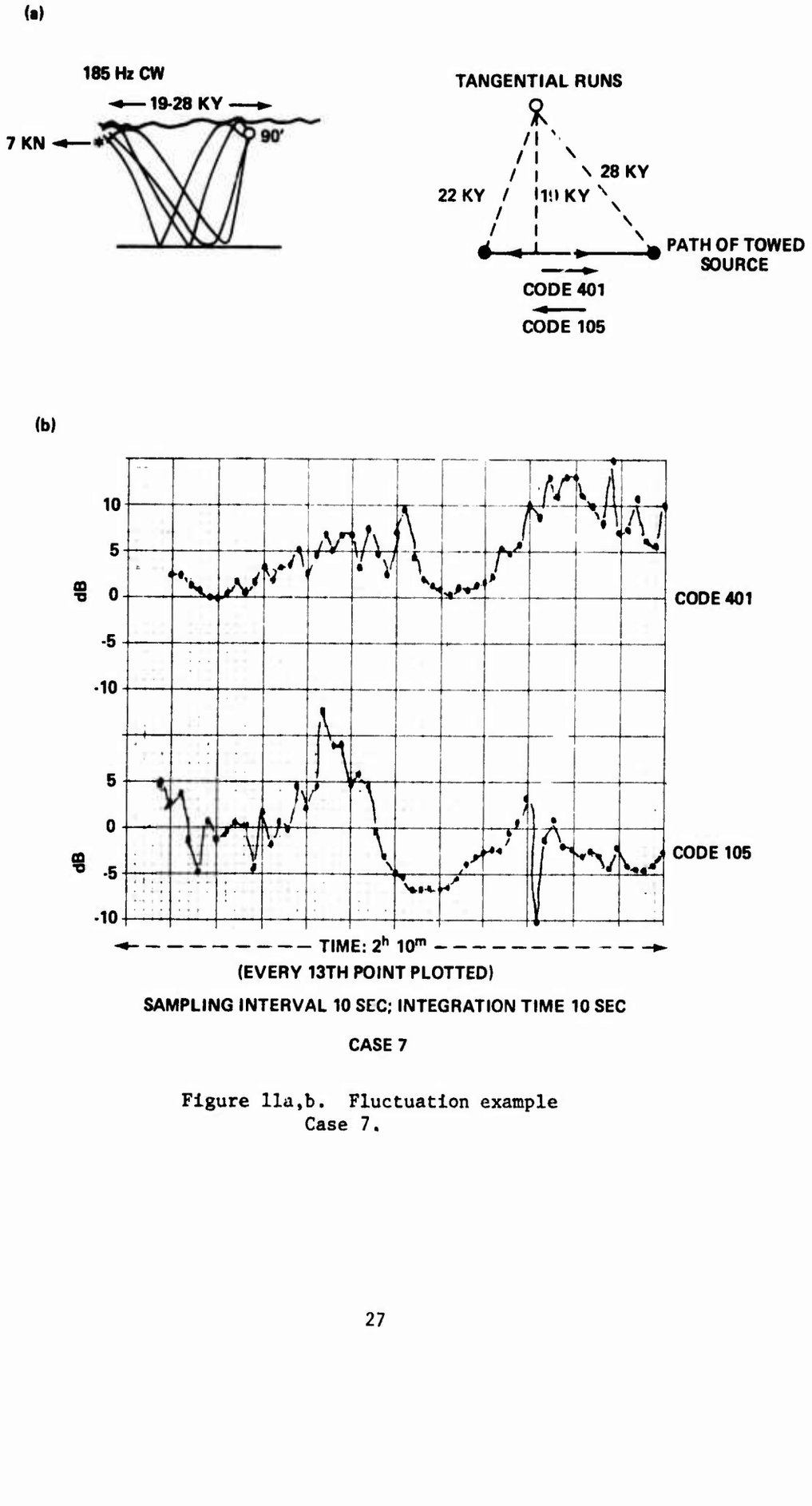

Figure 11a,b. Fluctuation example Case 7.

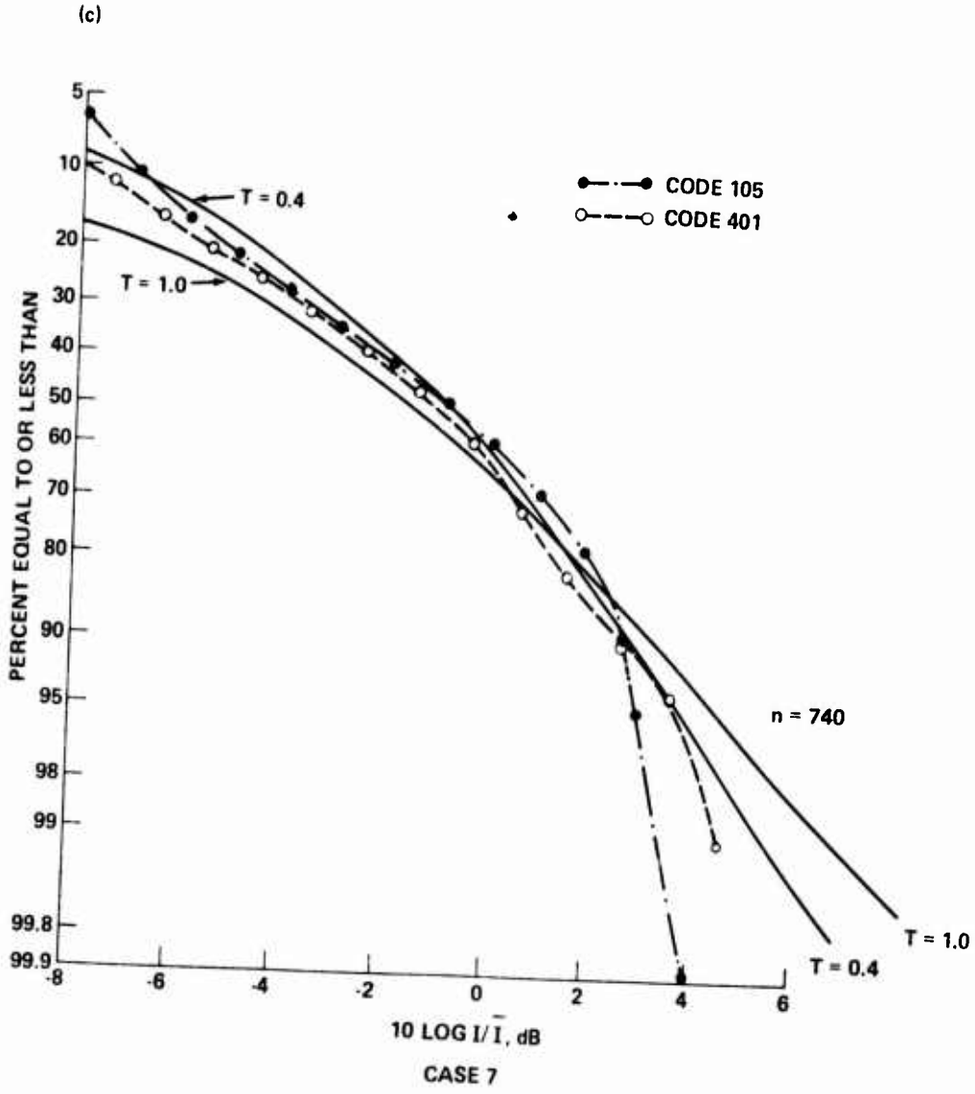

Figure 11c. Amplitude distribution, Case 7.

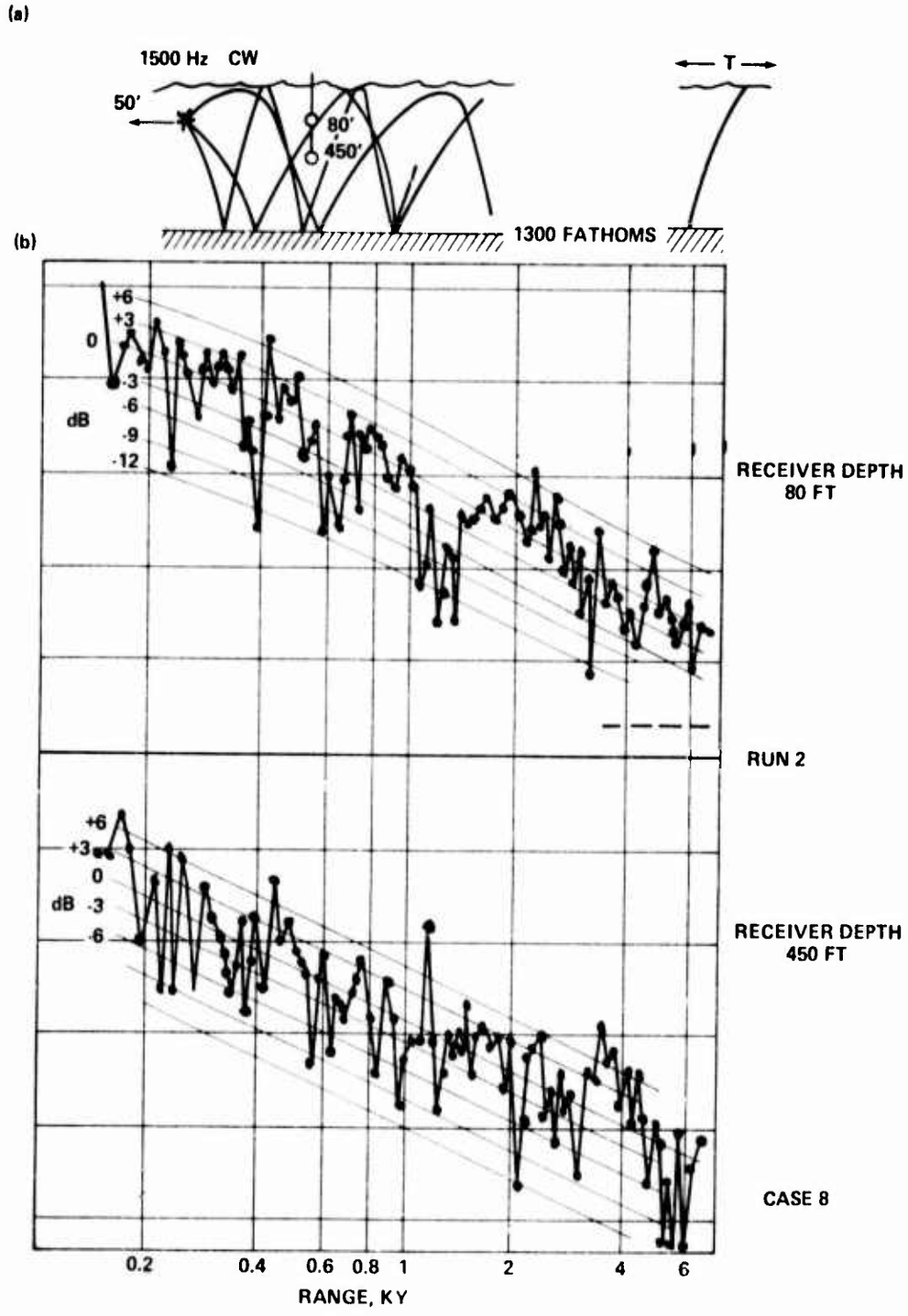

Figure 12a,b. Fluctuation example, Case 8.

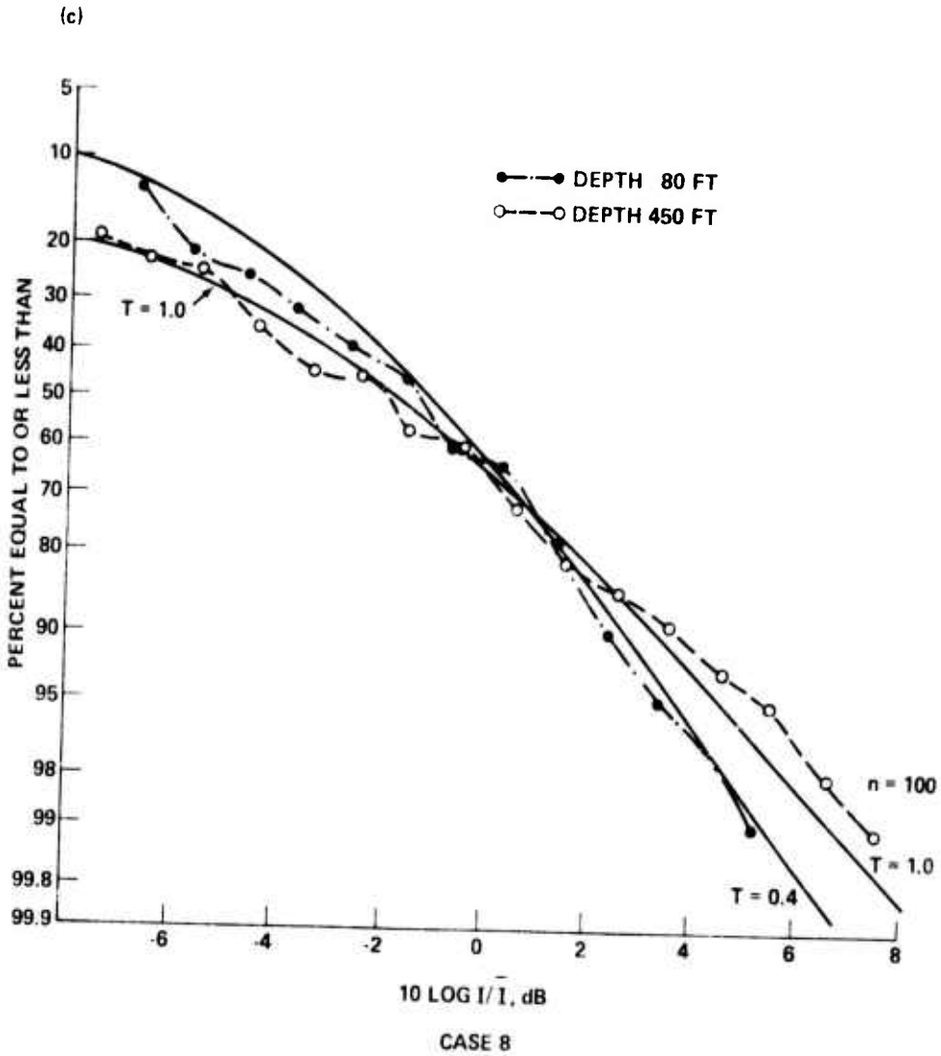

Figure 12c. Amplitude distribution, Case 8.

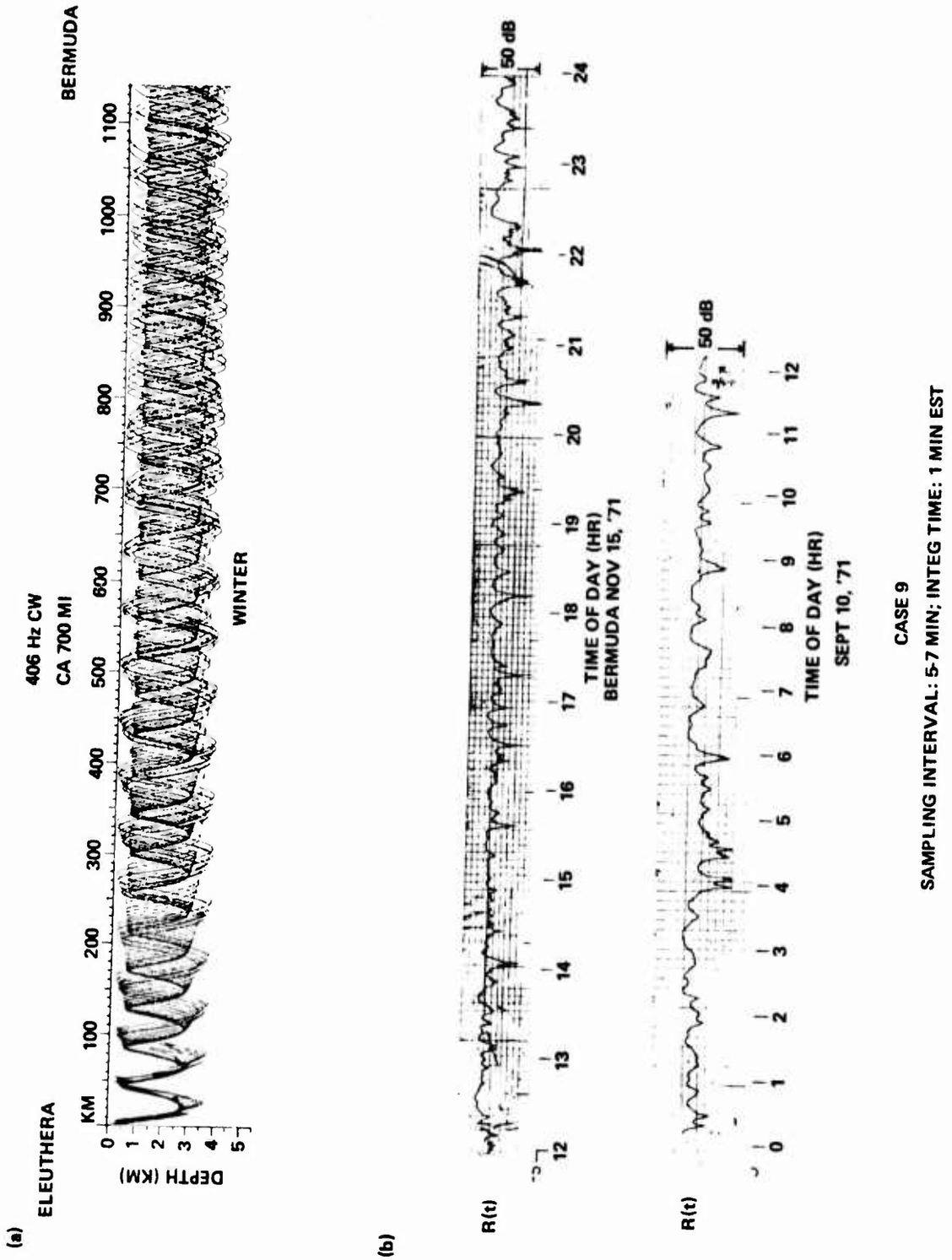

Figure 13a,b. Fluctuation example, Case 9.

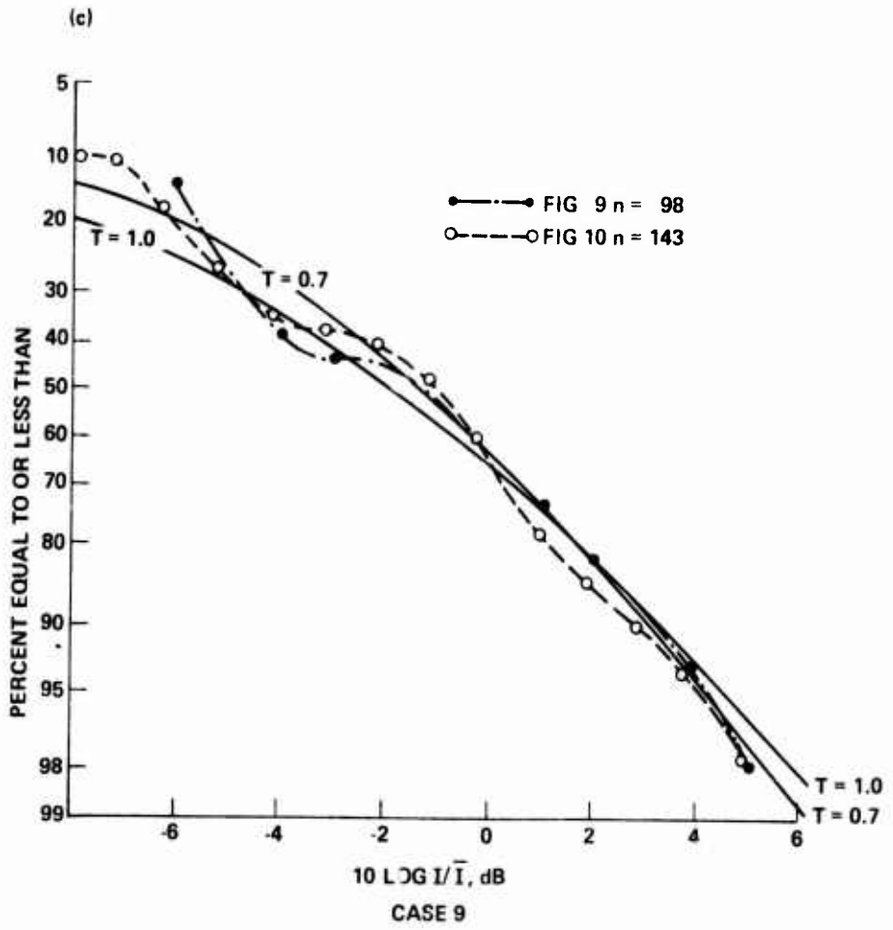

Figure 13c. Amplitude distribution, Case 9.

ELEUTHERA BERMUDA

367 Hz CW

(a) 711 mi

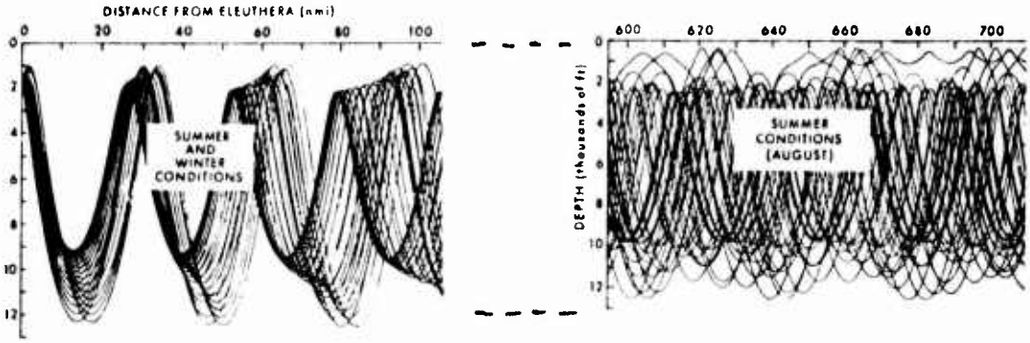

(b)

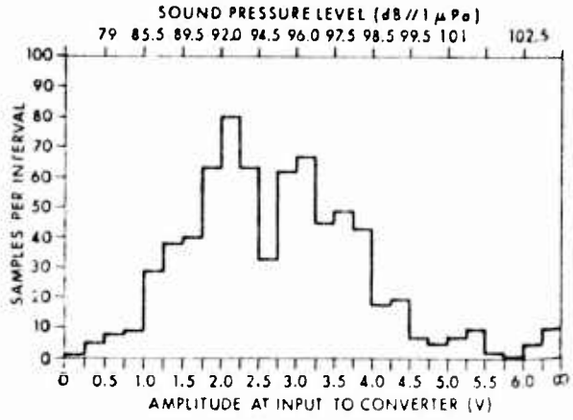

FIG. 9. Amplitude histogram for receiver 1-3U during July experiment. Total samples 720.

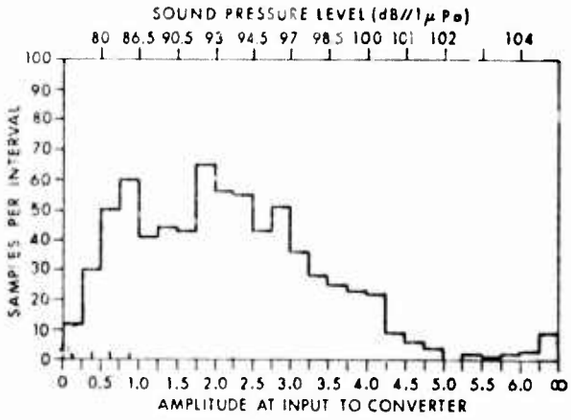

FIG. 10. Amplitude histogram for receiver 1-4U during July experiment. Total samples 720.

CASE 10

SAMPLING INTERVAL 15 SEC; INTEG. TIME 15 SEC

Figure 14a,b. Fluctuation example, Case 10.

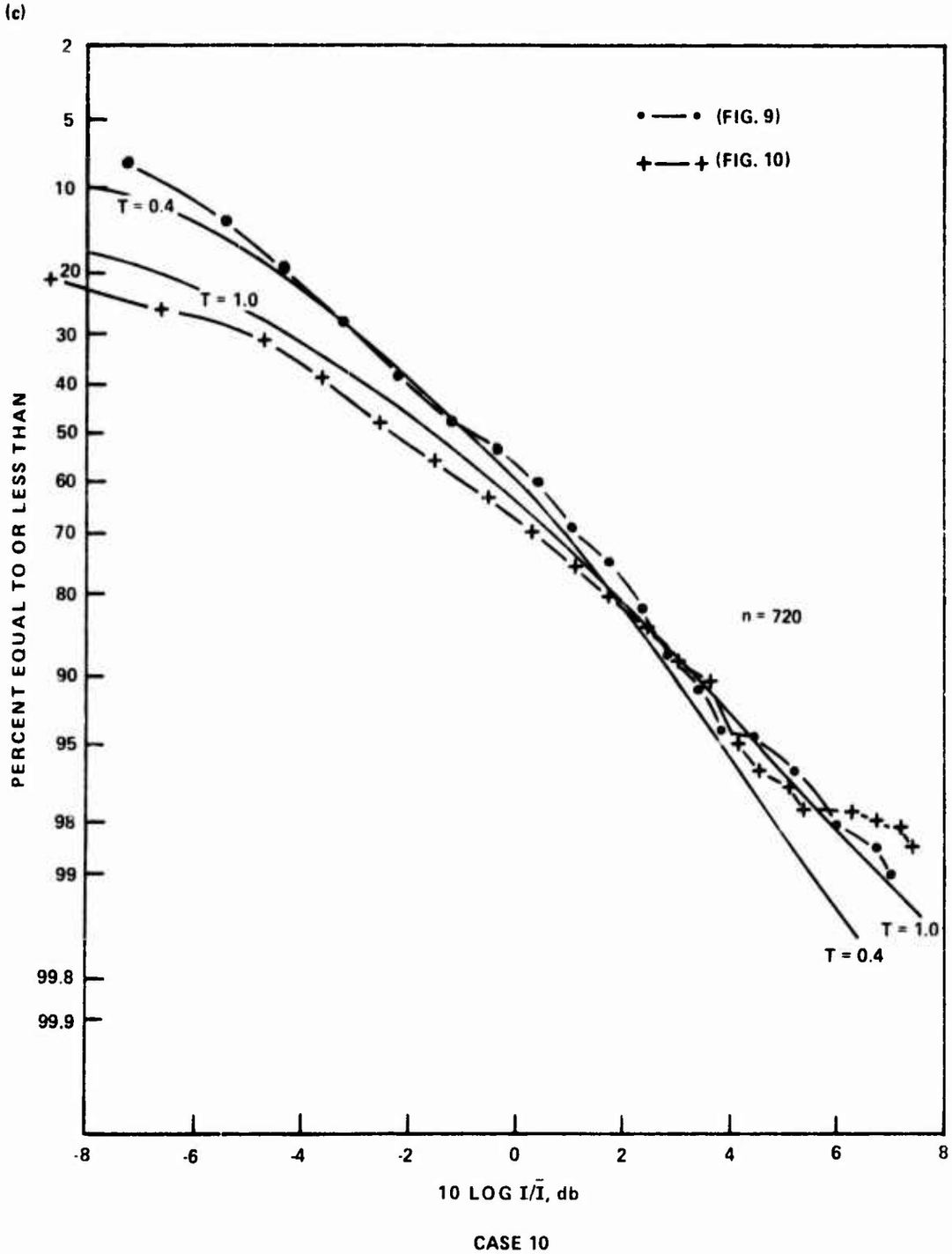

Figure 14c. Amplitude distribution, Case 10.

(a) 800 Hz, 5 ms PULSES

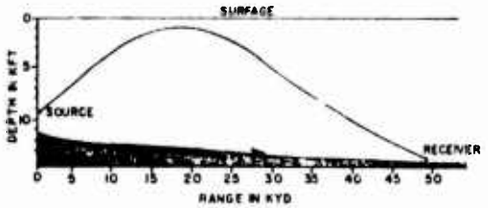

FIG. 1. Propagation path between sound source and receivers.

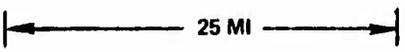

(b)

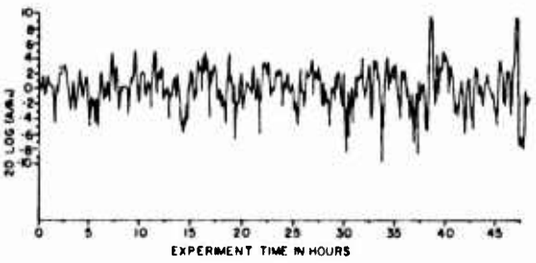

(a)

SAMPLING INTERVAL 6 MIN; INTEGRATION TIME 5 ms

CASE II

Figure 15a,b. Fluctuation example, Case 11.

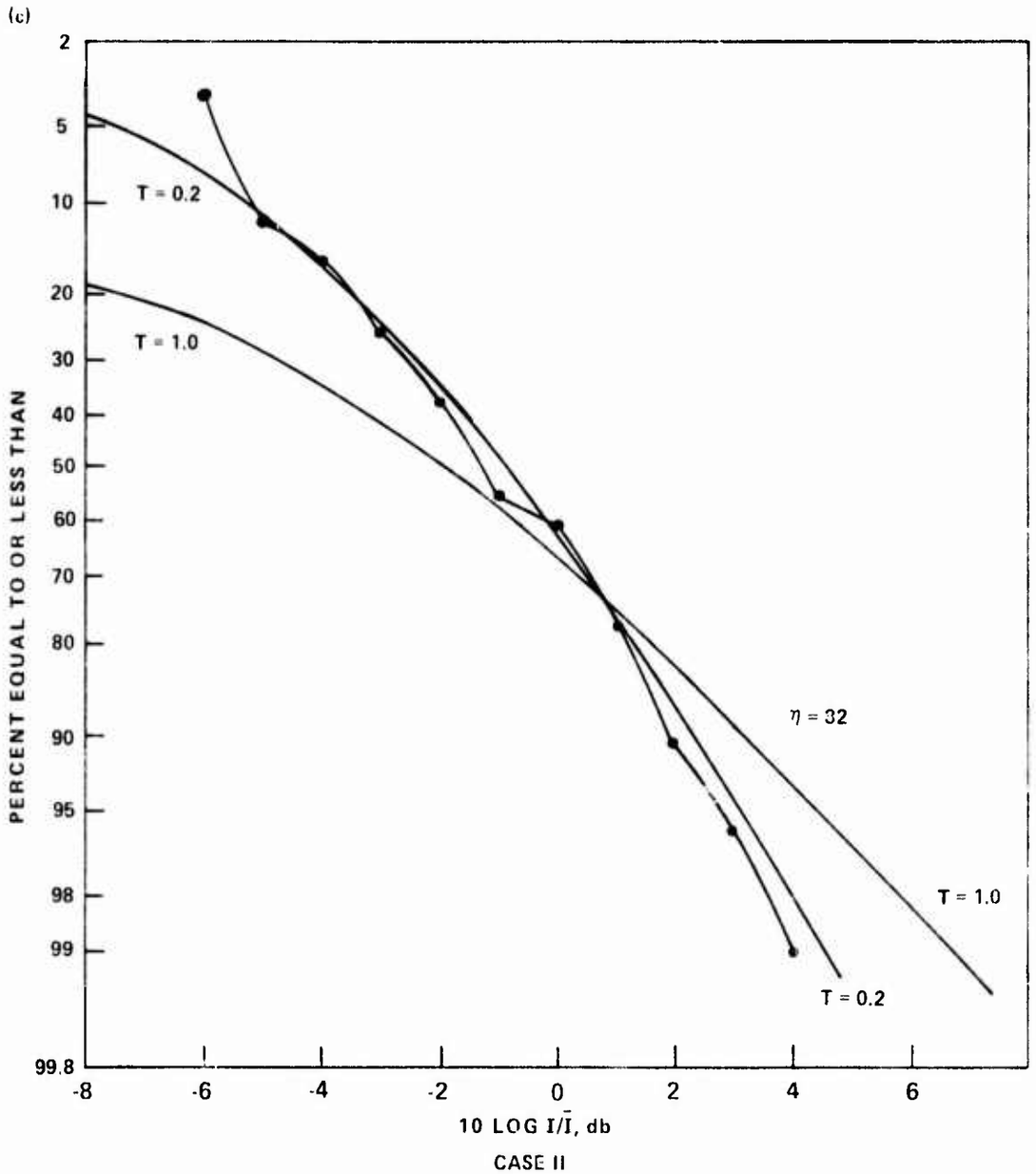

Figure 15c. Amplitude distribution, Case 11.

Table I: Experimental Conditions

Case	Propagation Mode	Frequency, kHz.	Source Depth, ft.	Rec. Depth ft.	Source Speed, kn.	Source-Rec. Range	Sampling Interval	Integration Time sec.	No. of Samples	Reference in Table II
1	Surface Duct	13.0	60	60,300	0	4 mi.	10 sec.	0.1	100	1
2	Surface Duct	1.12	50	60,300	5	11 ky.	1 sec.	0.2 approx.	100	1
3	Surface Duct Direct path	1. 12	50	1000,8000	0	5 mi.	1 sec.	0.1 approx.	100	2
4	Surface Duct	0.7,1.3, 3.0	90	80	?	4-32 ky	?	?	160	3
5	Bottom Bounce	0.142	85	60	3	Var.	Var.	Var.	100	4
6	Bottom Bounce	0.185	250	90	?	11-4 mi.	1 min.	10	58	5
7	Bottom Bounce	0.185	250	90	7	19-28 ky.	10 sec.	10	740	5
8	Bottom Bounce	1.5	50	80,450	6	0.2-5 ky.	6 sec. approx.	short	200	6
9	Refracted Paths	.376	deep	deep	0	700 mi.	5-7 min.	1 min. approx	98,143	7
10	Refracted Paths	.376	1729	5580	0	711	15 sec.	15 sec.	720	8
11	Single Refracted Path	.80	9500	14,100	0	24 min.	6 min.	5 ms.	82	9

Table II References for Table I

1. R. J. Urick, Amplitude Fluctuations of Sound Transmitted in the Surface Duct, NOLTR 74-130, 1974.

2. R. J. Urick, Coherence of Ambient Noise and the Signal from a Steady Source at Different Depths at a Deep Sea Location, NOLTR 73-68, 1973.

3. H. Eden and J. Nicol, Acoustic Transmission in an Ocean Surface Duct, J. Acoust. Soc. Am. 53, 819, 1973.

4. R. J. Urick, Amplitude Fluctuations of the Sound from a Low Frequency Moving Source in the Deep Sea, NOLTR 74-43, 1974.

5. Digitized data from a FIXWEX exercise provided by M. L. Higgins, Naval Air Development Center.

6. D. Stansfield, CW Propagation at 1.5kc/s in Deep Water, H. M. Underwater Detection Establishment, Pamphlet 641, 1959 (unpublished).

7. J. G. Clark and M. Kronengold, Long Period Fluctuations of CW Signals in Deep and Shallow Water, Institute for Acoustical Research, Project MIMI Interim Report, 1, 1974.

8. G. E. Stanford, Low-frequency Fluctuations of a CW Signal in the Ocean, J. Acoust. Soc. Am 55, 968, 1974.

9. R. M. Kennedy, Phase and Amplitude Fluctuations in Propagating Through a Layered Ocean, J. Acoust. Soc. Am. 46, 737, 1969